Int. J. Cancer: **124,** 2210–2219 (2009)

In vitro and *in vivo* study of phloretin-induced apoptosis in human liver cancer cells involving inhibition of type II glucose transporter

Chih-Hsiung Wu[1,2], Yuan-Soon Ho[3], Chia-Yi Tsai[4], Ying-Jan Wang[5], How Tseng[6], Po-Li Wei[1,2], Chia-Hwa Lee[3], Ren-Shyan Liu[7] and Shyr-Yi Lin[8,9]*

[1]*Graduate Institute of Clinical Medicine, Taipei Medical University Hospital, Taipei Medical University, Taipei, Taiwan*
[2]*Department of Surgery, Taipei Medical University Hospital, Taipei Medical University, Taipei, Taiwan*
[3]*Graduate Institute of Biomedical Technology, Taipei Medical University, Taipei, Taiwan*
[4]*Division of Transfusion Medicine, Department of Pathology and Laboratory Medicine, Shin Kong Wu Ho-Su Memorial Hospital Taipei, Taiwan*
[5]*Department of Environmental and Occupational Health, National Cheng Kung University Medical College, Tainan, Taiwan*
[6]*Graduate Institute of Medical Sciences, Taipei Medical University, Taipei, Taiwan*
[7]*Department of Nuclear Medicine, Veterans General Hospital, Taipei, Taiwan*
[8]*Department of Internal Medicine and Primary Care Medicine, School of Medicine, Taipei Medical University and Hospital, Taipei, Taiwan*
[9]*Cancer Research Center, Taipei Medical University Hospital, Taipei, Taiwan*

Phloretin (Ph), a natural product found in apples and pears with glucose transporter (GLUT) inhibitory activity, exerts antitumor effects. However, little is known about its effects on human liver cancer. The purpose of this study is to test the cytotoxic effects of Ph on HepG2 cells and to identify the underlying molecular pathways. Human hepatocellular carcinoma specimens and HepG2 show a high level of GLUT2 transporter activity in the cell membrane. Real-time PCR and MTT assays demonstrate that Ph-induced cytotoxicity correlates with the expression of GLUT2. Flow cytometry and DNA fragmentation studies show that 200 μM Ph induces apoptosis in HepG2, which was reversed by glucose pretreatment. GLUT2 siRNA knockdown induced HepG2 apoptosis, which was not reversed by glucose. Western blot analysis demonstrates that both intrinsic and extrinsic apoptotic pathways in addition to Akt and Bcl-2 family signaling pathways are involved in Ph-induced cell death in HepG2 cells. Furthermore, using flow cytometry analysis, a mitochondrial membrane potential assay and Western blot analysis, we show that cytochalasin B, a glucose transport inhibitor, enhances the Ph-induced apoptotic effect on HepG2 cells, which was reversed by pretreatment with glucose. Furthermore, we found significant antitumor effects *in vivo* by administering Ph at 10 mg/kg intraperitoneally to severe combined immune deficiency mice carrying a HepG2 xenograft. A microPET study in the HepG2 tumor-bearing mice showed a 10-fold decrease in ^{18}F-FDG uptake in Ph-treated tumors compared to controls. Taken together, these results suggest that Ph-induced apoptosis in HepG2 cells involves inhibition of GLUT2 glucose transport mechanisms.

Key words: apoptosis; glucose transporter; HepG2 cell; phloretin; hepatocellular carcinoma

Consumption of apples has been associated with prevention of cancer and chronic diseases.[1,2] The phytochemicals found in apples have potent antioxidant activity and antiproliferative effects on cancer cells.[3–5] Ph is a dihydrochalcone found in apples and other fruits,[6] which is known to suppress both transmembrane glucose transport[7] and inhibition of protein kinase C.[8] Ph has been shown to inhibit human leukemia cell growth[9] and to induce apoptosis of melanoma cells by suppressing transmembrane glucose transport.[6] Ph also inhibits the growth of bladder cancer and rat mammary adenocarcinoma cells *in vivo*.[10] These *in vitro* and *in vivo* findings suggest that Ph has antitumor activity. However, little is known about the effects of Ph on human hepatoma cells.

Facilitated glucose transporters (GLUTs) mediate the energy-independent transport of glucose across the plasma membrane.[11] Thirteen GLUTs have been identified and classified into 3 groups according to their sequence similarities and characteristics.[12] The GLUTs have tissue-specific patterns of expression reflecting the various glucose requirements of different tissues.[13] GLUT2, for example, is distributed in liver cells, pancreatic islet β-cells, intestinal epithelial cells and kidney proximal renal tubule cells.[14,15] Malignant cells have been shown to express high levels of glucose transporters in connection with an enhanced rate of glycolysis.[16] Increased glucose uptake in hepatocellular carcinoma (HCC) compared with adjacent nontumoral liver tissue has been documented,[17–19] and previous reports demonstrated that GLUT2 mRNA expression was increased in human liver tumors compared with nontumorous liver tissue,[20] while no expression of GLUT1 was detected in normal human liver tissue, adenoma, or HCC.[17,21] These findings suggest that GLUT2 expression is important in HCC tumorigenesis.

Recent reports suggest that the suppression of glucose transport is linked to the earliest steps of apoptosis.[22] Glucose deprivation may induce 3 major pathways, including the ATP depletion-induced mitochondrial death pathway, the oxidative stress-related cell death pathway, and induction of hypoxia-inducible factor-1α with concomitant activation of the p53-induced cell death pathway.[22] It has been suggested that Ph is a specific GLUT2 inhibitor.[23,24] In the present study, we demonstrate that human HCC and hepatoma cells express high levels of GLUT2. Treatment with Ph induces apoptosis in HepG2 cells which depends on GLUT2 expression and suppresses liver tumor growth in a xenograft mouse model. Both of these effects involve suppression of glucose transport.

Material and methods

Cell culture, chemicals and patient samples

The malignant human cell line HepG2 (HB-8065, American Type Culture Collection) was derived from a human hepatoma. The cells were grown in Eagle's minimal essential medium sup-

Abbreviations: ^{18}F-FDG, ^{18}F-fluorodeoxyglucose; DMEM, Dulbecco's modified Eagle's medium; DMSO, Dimethyl sulfoxide; FACS, fluorescence-activated cell sorting; FCS, fetal calf serum; GLUT, glucose transporter; GUS, β-glucuronidase; HCC, hepatocellular carcinoma; MTT, 3-(4,5-dimethylthiazol-2-yl)-2,5-diphenyl-2H-tetrazolium bromide; PARP, poly-ADP-ribose polymerase; Ph, phloretin; PKC, protein kinase C; SCID, severe combined immune deficiency.

The first two authors contributed equally to this work.

Grant sponsor: The National Science Council of Taiwan; Grant numbers: NSC 95-2320-B-038-011, NSC 95-2314-B-038-006, NSC 96-2317-B-038-001.

***Correspondence to:** Department of Internal Medicine, School of Medicine, Taipei Medical University Hospital, 252 Wu-Hsing Street, Taipei 110, Taiwan. Fax: 886-2-27393422. E-mail: sylin@tmu.edu.tw

Received 19 May 2008; Accepted after revision 19 November 2008
DOI 10.1002/ijc.24189
Published online 26 November 2008 in Wiley InterScience (www.interscience.wiley.com).

plemented with 10% fetal calf serum (FCS), penicillin (100 U/ml), streptomycin (100 μM/ml) and 0.3 mg/ml glutamine in a humidified incubator (37°C, 5% CO_2). Ph (Sigma Chemical, St. Louis, MO) dissolved in 0.05% dimethylsulfoxide (DMSO) was added at the doses indicated. For control specimens, the same volume of 0.05% DMSO without Ph was added.

The cells used for determining GLUT2 expression were as follows: CA9-22, oral cancer; FHC, normal colon cell; A431, epidermoid carcinoma; Hep3B, hepatocellular carcinoma; MCF-10A, mammary gland epithelial fibrocystic cell; LNCAP, prostate carcinoma; COLO 205, colorectal adenocarcinoma; AU565, breast adenocarcinoma; CL (Calu-1), lung epidermoid carcinoma; RAW, macrophage leukemia; HT 29, colorectal adenocarcinoma; NIH3T3, mouse embryo fibroblast; COLO-DLD, colorectal adenocarcinoma; MCF-7, breast adenocarcinoma; PC3, prostate adenocarcinoma; HBL 100, breast-derived nonmalignant cell; A549, lung carcinoma; KA, keratoacanthoma; MB231, breast adenocarcinoma; HL60, promyeloblastic leukemia; MCEC, murine cardiac endothelial cell; U373, human astrocytoma. The cells were grown and routinely maintained in the following media: minimal essential medium (for Hep3B, MCF-7, CL, KA), Dulbecco's modified Eagle's medium (DMEM) (for CA9-22, A431, RAW, NIH3T3, A549, MCEC, U373), DMEM-F12 (for FHC, MCF-10A, MB231), and RPMI-1640 (for LNCAP, COLO 205, HT 29, AU565, COLO-DLD, PC3, HBL 100, HL 60). In all cases, the medium was supplemented with 10% FCS, 2 mM L-glutamine, 100 units/ml penicillin and 100 mg/ml streptomycin. Cells wee incubated at 37°C in a 5% CO_2 atmosphere incubator.

Human HCC samples ($n = 14$) were obtained as anonymous specimens from Taipei Medical University Hospital through the protocol approved by the Institutional Review Board (P950023) and were embedded in paraffin for immunohistochemistry. There are 12 male patients with mean age of 56.4 years (range, 39–77 years); 2 female patients with mean age of 57.5 years (53 and 62 years). Among the 14 patients, 9 of them are hepatitis B carrier; 2 of them are hepatitis C carrier; 1 patient has simultaneous hepatitis B and C infection; 2 of them are free of hepatitis B and C infection. Two of the patients also present history of heavy alcohol drinking, one is hepatitis B and the other is hepatitis C carrier.

Immunofluorescence assay

Human HepG2 cells were immunostained for 2 hr with 1:100 dilutions of monoclonal antiGLUT2 or anticaveolin antibodies (Santa Cruz Biotechnology, CA). After washing with PBS/Tween 20 three times, the monoclonal antibody was visualized with fluorescent-conjugated secondary antibodies (FITC and rhodamine) diluted 1:50 in blocking buffer for 1 hr. Coverslips were washed, mounted, and viewed under a Leica TCS SP5 confocal laser-scanning microscope (Leica Microsystems, Heidelberg, Germany).

Immunohistochemistry study

As described previously,[25] paraffin-embedded blocks were sectioned at 5–7-μm thickness. After microwave pretreatment in citrate buffer (pH 6.0) for antigen retrieval, slides were immersed in 0.3% hydrogen peroxide for 20 min to block the endogenous peroxidase activity. After intensive washing with PBS, slides were incubated overnight at 4°C with the anti-GLUT2 antibody at a dilution of 1:100. After incubation with a biotinylated secondary antibody (1:200), slides were incubated with peroxidase-conjugated streptavidin (DAKO LSAB+kit; Dako, Carpinteria, CA). Reaction products were visualized by immersing slides in diaminobenzidine tetrachloride, and finally were counterstained with hematoxylin. As for the negative controls, sections were stained as above but with PBS substituted for the primary antibody.

mRNA detection using real-time PCR

Total RNA was extracted from cells using phenol chloroform extraction (TRIzol Reagent, Invitrogen, Carlsbad, CA). Primers for GLUT2 were the following: forward, 5′-AGTTAGATGAGGA AGTCAAAGCAA-3′; reverse, 5′-TAGGCTGTCGGTAGCTGG-3′. These primers yielded an amplicon of 164 bp. Primers for β-glucuronidase (GUS) (forward 5′-AGTGTTCCCTGCTAGAA TAGATG-3′ and reverse 5′-AAACAGCCCGTTTACTTGAG-3′) were used to establish baseline mRNA content. A LightCycler thermocycler was used to conduct real-time PCR (Roche Molecular Biochemicals, Mannheim, Germany). Reaction reagents were purchased in a preformatted kit (LightCycler FastStart DNA Master SYBR Green I; Roche Diagnostics GmbH, Roche Molecular Biochemicals, Mannheim, Germany) containing 10× concentrations of Taq DNA polymerase, deoxynucleoside triphosphates, 10 mM $MgCl_2$, SYBR Green I and reaction buffer. Cycling conditions were as follows: denaturation at 95°C for 10 min, followed by 40 cycles with denaturation at 95°C for 5 sec, primer annealing at 60°C for 5 sec, and a single fluorescence acquisition step during amplicon extension at 72°C for 10 sec. Data were analyzed by Roche LightCycler Software version 4. DNA amount was determined by the standard curve method with background subtraction. A cycle of melting curve analysis for each PCR product was performed to detect primer dimers. Results are expressed as copy number of GLUT2 per μg of mRNA loaded.

3-(4,5-Dimethylthiazol-2-yl)-2,5-diphenyl-2H-tetrazolium bromide assay

The 3-(4,5-Dimethylthiazol-2-yl)-2,5-diphenyl-2H-tetrazolium bromide (MTT) assay was performed as described previously.[26] Cells were seeded in a 96-well plate at a density of 1×10^4 cells/well and allowed to adhere overnight. After removing the medium, 200 μl of fresh medium containing 10 mmol/l HEPES (pH 7.4) was added to each well. Then, 50 μl of MTT was added to the wells, and the plate was incubated for 2–4 hr at 37°C in the dark. The medium was removed, and 200 μl of DMSO and 25 μl of Sorensens's glycine buffer were added to the wells. Absorbance was measured using an ELISA plate reader at 570 nm with background subtraction at 650 nm.

Flow cytometry analysis

The cell cycle stages in the Ph- and DMSO-treated groups were measured by flow cytometry as previously described.[26] Cells were harvested and stained with a reagent containing propidium iodide (50 μg/ml) and DNase-free RNase (2 U/ml). Measurement of nuclear DNA was performed using fluorescence-activated cell sorting (FACS). The population of nuclei in each phase of the cell cycle was determined using CellFIT DNA analysis software (Becton-Dickinson, San Jose, CA), and 15,000 events were analyzed for each sample.

Analysis of DNA fragmentation

Analysis of DNA fragmentation was performed as previously described.[26] Briefly, Ph- and DMSO-treated cells were seeded in 100-mm dishes. The DNA was extracted twice with equal volumes of phenol and once with chloroform-isoamyl alcohol (24:1, v:v), precipitated with 0.1 volume of sodium acetate (pH 4.8) and 2.5 volumes of ethanol at −20°C overnight, and finally was centrifuged at 13,000*g* for 1 hr. Genomic DNA was quantified, and equal amounts of DNA sample per lane were electrophoresed in a 2% agarose gel. The DNA was visualized by ethidium bromide staining.

Plasmids and transfection assays

We ablated GLUT2 expression in liver cancer cells with at least 2 independent small interfering RNAs (siRNAs). The target sequences of GLUT2 siRNA (5′-ACCAATTCCAGCTACCGAC-3′, 5′-GTCGGTAGCTGGAATTGGT-3′) were selected to suppress GLUT2 gene expression and GLUT2 scramble siRNA (scRNA) (5′-CAAGCGCAACTACCTATCC-3′, 5′-GGATAGG TAGTTGCGCTTG-3′) were used as controls. After BLAST analysis to verify that there was no significant sequence homology with other human genes, the selected sequence was inserted into a

BglII/HindIII-cut pSUPER vector to generate the pSUPER-glut2si and pSUPER-glut2sc vectors. All constructs were confirmed by DNA sequence analysis. The transfection protocol has been described previously.[27] Briefly, 5×10^6 cells were washed twice with PBS and mixed with 12 μg plasmid. We applied 1 pulse of 30 msec under a fixed voltage of 1.1 kV for HepG2 and 1 pulse of 40 msec under a fixed voltage of 1 kV for Hep3B cells on a pipette-type microporator MP-100 (Digital Bio, Seoul, Korea).

Western blot analysis

Western blot analysis was performed as described previously.[26,28] Monoclonal or polyclonal antibodies were obtained from various sources as indicated: anti-p53, anti-caspase 8, anti-Bax, anti-Bcl-2, anti-cytochrome c, anti-Bid, anti-Bad, anti-PARP, anti-AIF, anti-AKT, anti-survivin and anti-XIAP antibodies were purchased from Santa Cruz Biotechnology (Santa Cruz, CA); anti-caspase 9 and anti-caspase 3 antibodies from Stressgen Biotechnologies (Victoria, British Columbia, Canada); and anti-p-AKT from Cell Signaling Technology (Beverly, MA,). Briefly, cell lysates were prepared, electrotransferred, immunoblotted with antibodies, developed using the SuperSignal chemiluminescence kit as indicated by the manufacturer (Pierce Biotechnology, Rockford, IL) and visualized by autoradiography. Expression of GAPDH (Abcam, Cambridge, UK) was used as a control to test for equal protein loading.

Mitochondrial transmembrane potential assay

Mitochondrial transmembrane potential ($\Delta\Psi_m$) was determined as described previously.[28] Briefly, 5×10^5 cells were cultured in 10 cm dishes for 15 hr. After various treatments for 24 hr, the cells were harvested with 1× trypsin-EDTA and centrifuged in a 15 ml tube at 2,000 rpm for 5 min. After 2 washes with PBS, the cells were loaded with the cationic lipophilic fluorochrome, tetrachlorotetraethylbenzimidazol carbocyanine iodide (JC-1, 5 μg/ml), for 20 min at room temperature. Cells were washed twice with PBS and submitted to flow cytometry analysis. Active mitochondria with high $\Delta\Psi_m$ form JC-1 aggregates, which are red (FL2, 590 nm), whereas in mitochondria with low $\Delta\Psi_m$, JC-1 remains in a monomeric, green form (FL1, 527 nm). The ratio of red to green (FL2/FL1) reflects the change in $\Delta\Psi_m$.

Treatment of HepG2-derived xenografts in vivo

Male severe combined immune deficiency (SCID) mice (5–6-weeks old, purchased from National Science Council Animal Center, Taipei, Taiwan) were injected subcutaneously between the scapulae with 5×10^6 HepG2 cells in 0.2 ml PBS. After transplantation, tumor size was measured using calipers, and tumor volume was estimated according to the formula: tumor volume (mm^3) = $L \times W^2/2$, where L is the length and W is the width.[29] Once tumors reached a mean size of 200 mm^3, animals received intraperitoneal injections of either DMSO ($n = 5$) or 10 mg/kg Ph ($n = 5$) three times per week for 6 weeks. All animal studies were performed according to the local guidelines for animal care and protection.

MicroPET imaging

Following a previously described protocol,[30] microPET images of the HepG2 tumor-bearing mice were obtained using the R4 system (Concorde Microsystems, Knoxville, TN). MicroPET scanning was performed at 6 weeks after tumor implantation. On the day of imaging, DMSO ($n = 5$) and Ph-treated ($n = 5$) tumor-bearing mice were anesthetized with isoflurane (Abbott Laboratories, Queensborough, Kent, England) using a vaporizer system (A.M. Bickford, Wales Center, NY) and intravenously injected with ~14.8 MBq of ^{18}F-fluorodeoxyglucose (^{18}F-FDG) in 0.2 ml of saline through the lateral tail vein by bolus injection. Each mouse was imaged in the prone position. The mice were scanned for 10 min at each time point (30, 60, 90 and 120 min postinjection of the ^{18}F-FDG), with the long axis of the mouse parallel to the long axis of the scanner. All images were reconstructed using the ordered-subsets expectation maximization reconstruction method, with a 128 × 128 pixel image matrix, 16 subsets, 4 iterations, and use of a Gaussian filter. Transmission scanning was performed at 130 min postinjection. Acquisition time was 600 sec, and images were reconstructed using filtered backprojection.

Statistical analysis

Results are expressed as mean ± S.E. for each study. Comparisons were subjected to one-way analysis of variance (ANOVA) followed by the Student's *t*-test. Statistical significance was accepted at $p < 0.05$.

Results

Localization of GLUT2 transporter in HepG2 cells and human liver tissues and expression of GLUT2 mRNA in cell lines correlate with Ph cytotoxicity

We first examined the expression and localization of the GLUT2 transporter in HepG2 cells. Cells were immunostained with GLUT2 and caveolin-specific antibodies and analyzed by confocal microscopy. As shown in Figure1*a*, the yellowish dots in the cell membrane indicate the colocalization of GLUT2 and caveolin proteins, suggesting the presence of GLUT2 transporter in the HepG2 cell membrane. For human HCC and adjacent normal liver tissue, an immunohistochemistry study was performed. As shown in Figure 1*b*, the normal hepatocytes showed no apparent GLUT2 protein expression, whereas adjacent HCC tissue contained substantial GLUT2 protein expression in the cell membrane (arrows). We next analyzed GLUT2 mRNA expression in 23 primary cells or cell lines using real-time RT-PCR. As shown in Figure 1*c*, GLUT2 mRNA was highly expressed in HepG2 cells, followed by Hep3B cells. The remaining cells expressed a low level of GLUT2 mRNA. We then tested Ph, a GLUT2 inhibitor, for cytotoxic effects on cancerous and normal cells expressing either high or low levels of GLUT2. As shown in Figure 1*d*, treating HepG2 cells with 50–150 μM Ph for 48 hr in the MTT assay significantly suppressed cell viability in a dose-dependent manner. Treatment of Hep3B cells with 100–150 μM Ph for 48 hr showed significant suppression of cell viability in the MTT assay. However, the Ph-induced effect is less prominent for Hep3B as compared to HepG2 cells. In contrast, no significant effect was observed on normal breast epithelial cells (MCF 10A) or breast cancer cells (AU565), suggesting that the cytotoxicity of Ph correlates with expression of GLUT2.

GLUT2 was involved in the Ph-induced liver cancer cell death

To test the mechanisms of Ph-induced HepG2 cytotoxicity, flow cytometry analysis was performed as shown in Figure 2*a*. Treatment of HepG2 cells with 100 and 150 μM Ph for 24 hr slightly increased the populations in G0/G1 (64.99%) and G2/M (39.58%), respectively. In contrast, treatment of HepG2 cells with 200 μM Ph for 24 hr significantly induced HepG2 cell death, evidenced by an increase in the sub-G1 population to 21.55%. To further clarify the mechanism of HepG2 cell death induced by Ph, a DNA fragmentation assay was performed as shown in Figure 2*b*. Treatment of HepG2 cells with 200 μM Ph for 24 hr induced significant DNA ladder formation, suggesting apoptotic cell death.

Ph has been shown to competitively inhibit glucose transport into tumor cells. To test whether Ph-induced HepG2 cell death was associated with an interference with glucose transport, the flow cytometry study in Figure 2*c* was performed. Treatment of HepG2 cells with 200 μM Ph for 24 hr increased the sub-G1 population to 22.54%. However, as the glucose concentration increased from 20, to 50, then to 100 mM, the sub-G1 population decreased from 12.24%, to 7.56%, then to 5.69%, respectively, suggesting that Ph-induced HepG2 apoptosis involved suppression of glucose intake into the cells.

To confirm that GLUT2 is directly involved in the Ph-induced liver cancer cell death, siRNA knockdown of GLUT2 expression

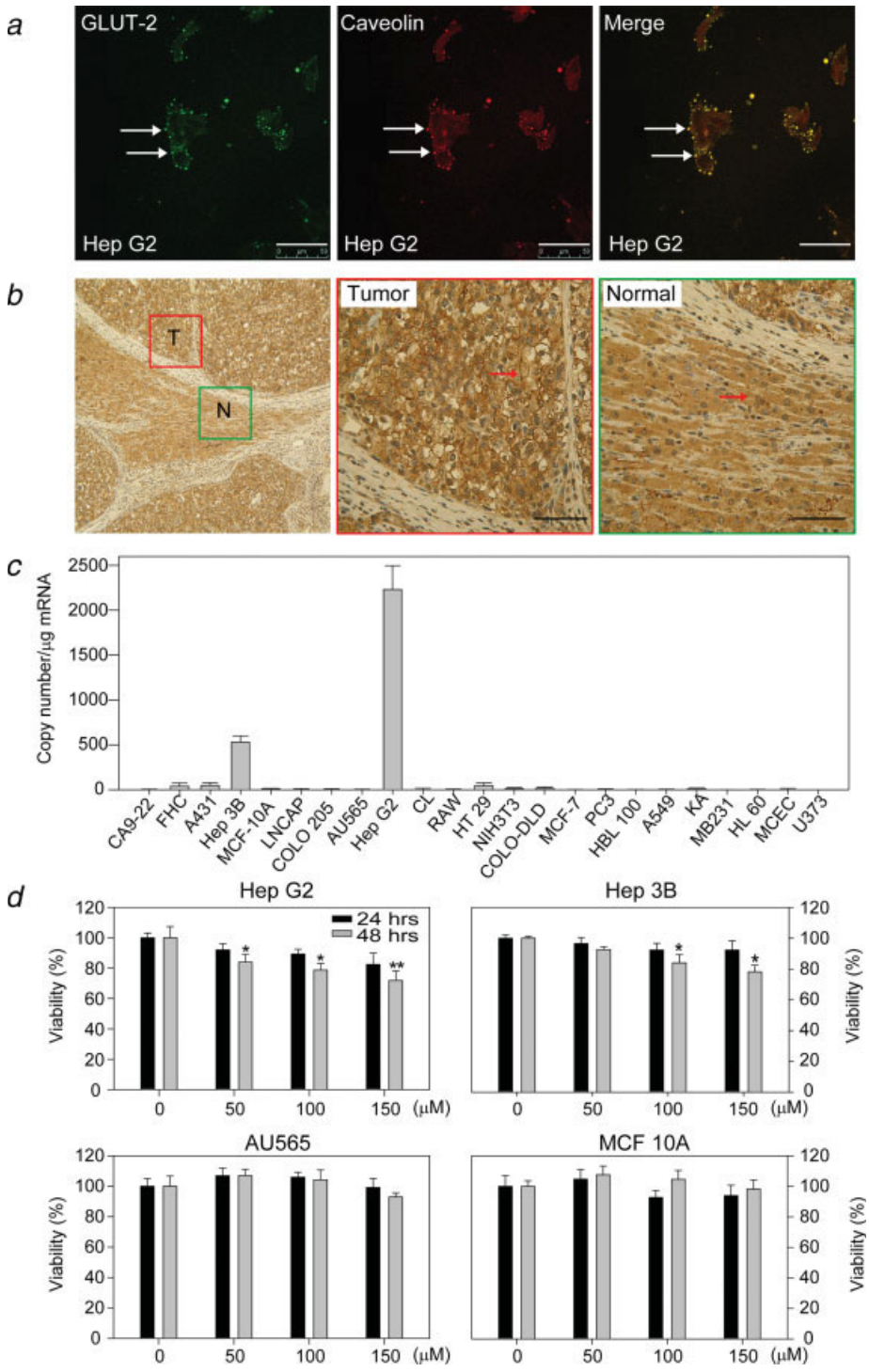

FIGURE 1 – Localization of the GLUT2 transporter in hepatoma cells and human HCC tissues, and Ph cytotoxicity correlated with the expression of GLUT2 mRNA in cell lines. (*a*) Confocal microscopic images of HepG2 cells. Immunocytochemistry was carried out using GLUT2 and caveolin-specific antibodies. Bar = 50 μm (*b*) Immunohistochemistry of GLUT2 expression in human HCC and adjacent nontumorous liver tissue. Bar = 150 μm (*c*) Real-time PCR of 23 primary cells or cell lines. RNA (2 μg) was reverse-transcribed for each cell population, and real-time PCR was performed. (*d*) HepG2, Hep3B, AU565, and MCF 10A cells were treated with Ph (50–150 μM) for 1 and 2 days. Dose-dependent suppression of cell viability was determined by an MTT assay. Four samples were analyzed in each group, and the results are presented as means ± SE. *, $p < 0.05$; **, $p < 0.01$ *vs*. DMSO (0 μM of Ph) control.

for HepG2 and Hep3B cells were used for further study (Fig. 2*d*). As shown in the left panel of flow cytometry, Figure 2*e*, similar sub-G1 population was induced for 200 μM Ph-treated HepG2 cells (the second bar) and GLUT2 siRNA knockdown HepG2 cells (the third bar). This effect cannot be further enhanced by treating GLUT2 siRNA knockdown HepG2 cells with Ph (the fourth bar). In contrast, scramble siRNA (the fifth bar) showed no significant effect to induce HepG2 apoptosis as compared to control. Interestingly, treatment of 100 mM glucose cannot reverse apoptotic effect in GLUT2 siRNA knockdown HepG2 cells (the sixth bar) suggesting a direct involvement of GLUT2 in the Ph-induced HepG2 cell death. Similar results were found for Hep3B as shown in the right panel of Figure 2*e*. But the effect of Ph-induced apoptosis in Hep3B cells was less prominent compared to HepG2 cells.

Both intrinsic and extrinsic apoptotic pathways are involved in Ph-induced apoptosis in HepG2 cells

Induction of apoptosis requires the activation of caspases.[31] Therefore, Western blot analysis was performed to investigate the involvement of caspase activation in Ph-induced apoptosis in

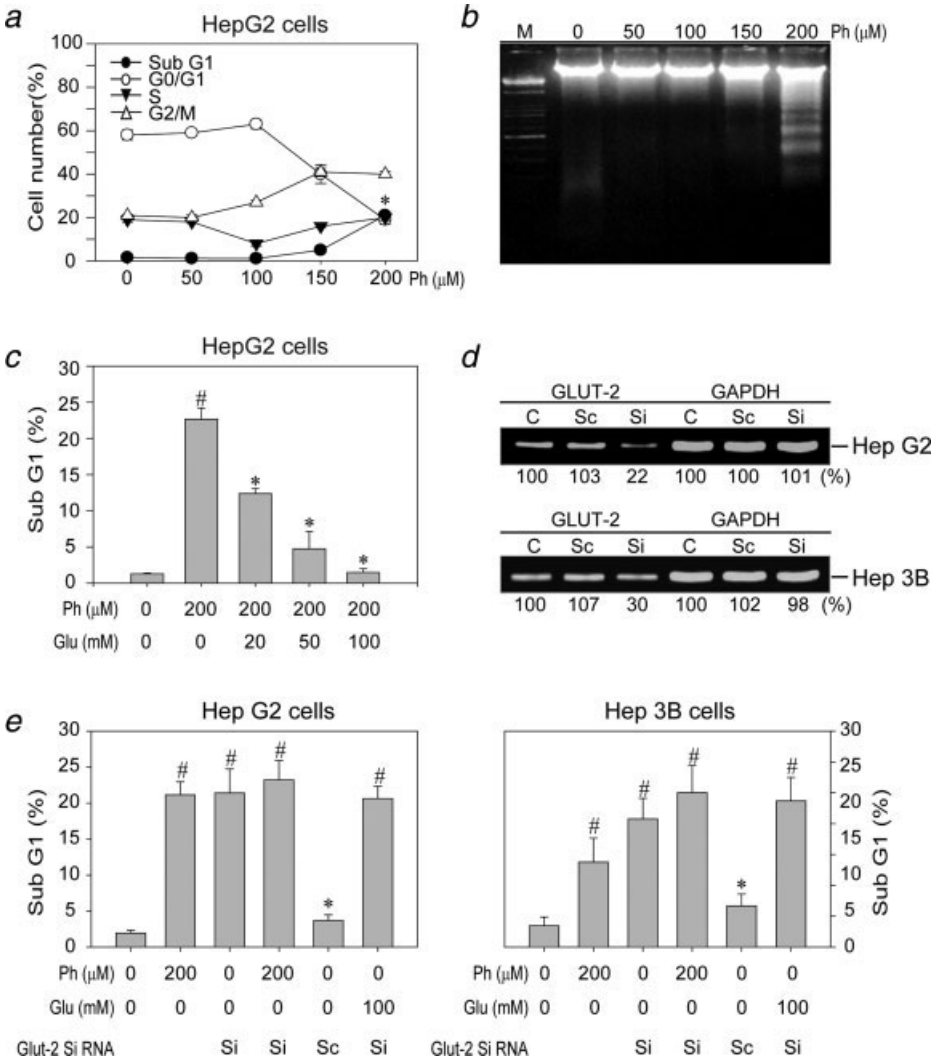

Figure 2 – Involvement of GLUT2 in the Ph-induced apoptosis in liver cancer cells (*a*) FACS analysis of DNA content was conducted after HepG2 cells were incubated for 24 hr in culture media supplemented with 10% FBS containing 0.05% DMSO (0 μM of Ph) control or Ph (50–200 μM in 0.05% DMSO). Four samples were analyzed in each group, and the results are presented as means ± SE. *, $p < 0.05$ *vs*. DMSO control. (*b*) DNA fragmentation assay in HepG2 cells. Cells were treated with Ph (50–200 μM) or 0.05% DMSO (0 μM of Ph) control, and DNA fragmentation was assessed 24 hr later. M, molecular weight markers. (*c*) FACS analysis of subG1 content after HepG2 cells were incubated in culture media supplemented with 10% FBS containing Ph (0 or 200 μM in 0.05% DMSO) with glucose (0–100 mM) for 24 hr. Four samples were analyzed in each group, and the results are presented as means ± SE.#, $p < 0.05$ *vs*. DMSO (0 μM of Ph) control; *, $p < 0.05$ *vs*. 200 μM Ph. (*d*) RT-PCR results of GLUT2 knockdown HepG2 and Hep3B cells. HepG2 or Hep3B cells were transfected with GLUT2 siRNA (Si) or scramble RNA (Sc) or untreated control (C) liver cancer cells for 24 hr. The number in percentage indicated the expression level compared to control. (*e*) FACS analysis of subG1 content after HepG2 (left panel) or Hep 3B (right panel) cells were incubated in culture media supplemented with 10% FBS containing Ph (0 or 200 μM in 0.05% DMSO), GLUT2 siRNA knockdown HepG2 or Hep3B, 200 μM of Ph together with GLUT2 siRNA knockdown HepG2 or Hep3B, GLUT2 scramble control HepG2 or Hep 3B, and glucose 100 mM together with GLUT2 siRNA knockdown HepG2 or Hep3B for 24 hr. Four samples were analyzed in each group, and the results are presented as means ± SE.#, $p < 0.05$ *vs*. DMSO (0 μM of Ph) control; *, $p < 0.05$ *vs*. GLUT2 siRNA knockdown liver cancer cells.

HepG2 cells. Treatment of HepG2 cells with 200 μM Ph activated caspase 3, as evidenced by a decrease in the level of procaspase 3 protein and the appearance of the cleaved form of caspase 3, and degradation of the caspase 3 substrate, poly-ADP-ribose polymerase (PARP). The addition of glucose at concentrations ranging from 20 to 100 mM reversed the activation of caspase 3 (Fig. 3*a*). To further elucidate the apoptotic pathways involved in the activation of caspase 3, we examined changes in the levels of caspases 8 and 9 proteins in the Ph-treated HepG2 cells. Treatment of HepG2 cells with 200 μM Ph activated caspases 8 and 9, as evidenced by the disappearance of procaspases 8 and 9, as well as the appearance of their cleaved forms. The addition of glucose at concentrations ranging from 20 to 100 mM reversed the activation of caspases 8 and 9 (Fig. 3*a*). These findings suggest that caspases 3, 8 and 9 are involved in Ph-induced apoptosis in HepG2 cells, and that the process depends on extracellular glucose concentration.

Activation of caspase 9 occurs during the release of cytochrome c from mitochondria into the cytosol. To test whether this release occurred in Ph-induced apoptosis in HepG2 cells, cytochrome c translocation was examined. As shown in Figure 3*b*, treatment of HepG2 cells with 200 μM Ph induced translocation of cytochrome c from the mitochondria into the cytosol. The addition of glucose at concentrations ranging from 20 to 100 mM reversed this translocation. Proteins of the Bcl-2 family are also involved in the control of apoptosis by regulating cytochrome c release. As shown in Figure 3*b*, treatment of HepG2 cells with 200 μM Ph induced

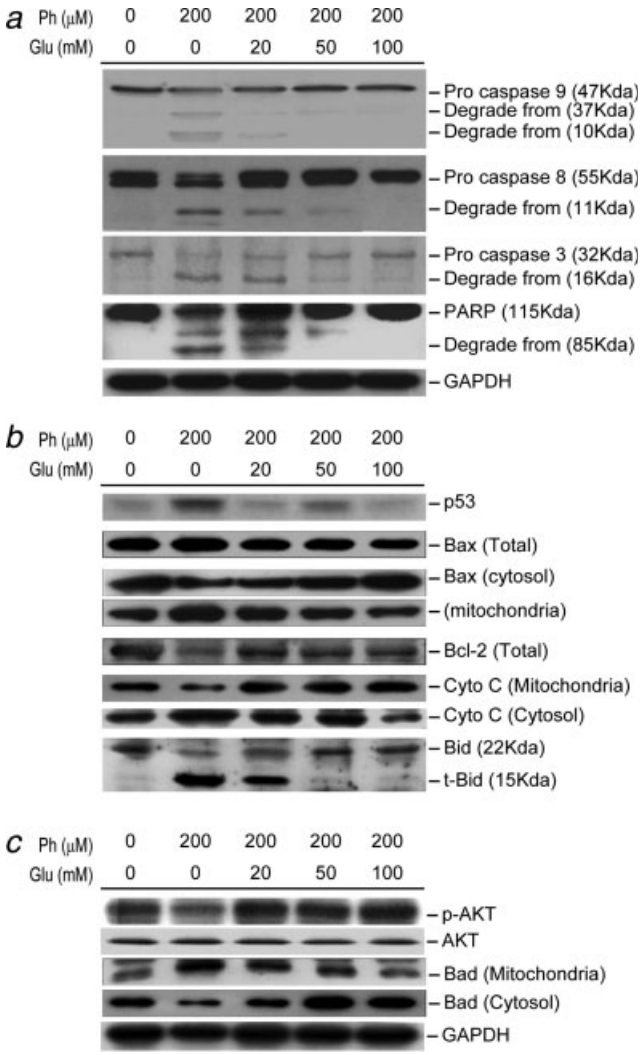

FIGURE 3 – Ph-induced effects on apoptotic regulatory proteins in HepG2 cells and reversal of these effects by glucose. Cells were incubated in culture medium supplemented with 10% FCS and 0.05% DMSO with or without Ph (200 and 0 μM), and with various concentrations of glucose (0–100 mM) for 24 hr. (*a*) Caspase 3, 8 and 9 pathways. (*b*) p53, Bcl-2 family and mitochondrial pathways. (*c*) Akt pathways. The cells were harvested, and protein extracts (100 μg per lane) were separated by SDS-PAGE. After electrophoresis, proteins were transferred onto Immobilon-P membranes, probed with the proper dilution of specific antibodies, and detected using the enhanced chemiluminescence method. The membrane was also probed with anti-GADPH antibody to correct for differences in protein loading.

translocation of Bax from the cytosol to mitochondria. It also increased expression of the Bax upstream regulator p53 protein and decreased expression of Bcl-2 protein. The addition of glucose at concentrations ranging from 20 to 100 mM reversed these effects. The proapoptotic protein Bid can be activated by caspase 8, leading to the formation of truncated Bid, which is subsequently translocated to the mitochondria during the activation of apoptosis. As shown in Figure 3*b*, treatment of HepG2 cells with 200 μM Ph induced Bid activation, leading to the formation of truncated Bid, which was reversed by the addition of glucose at concentrations ranging from 20 to 100 mM. These findings suggest that Bax, Bcl-2 and Bid proteins are all involved in Ph-induced apoptosis in HepG2 cells.

Akt activation can phosphorylate Bad, which leads to its inactivation through binding of a 14-3-3 protein. As shown in Figure 3*c*, treatment of HepG2 cells with 200 μM Ph inhibited Akt activation, evidenced by its decreased phosphorylation. It also activated Bad, as evidenced by the protein's translocation from the cytosol to the mitochondria. The addition of glucose at concentrations ranging from 20 to 100 mM reversed these effects. These findings suggest that Akt-Bad pathways are involved in Ph-induced apoptosis in HepG2 cells.

Cytochalasin B enhances Ph-induced apoptosis in HepG2 cells

Cytochalasin B is a glucose transporter inhibitor and has been shown to regulate a specific glucose-sensitive binding site in liver plasma membrane.[32] We tested the cytotoxic effects of cytochalasin B alone or in combination with Ph on HepG2 cells using a flow cytometry assay. As shown in Figure 4*a*, treatment of HepG2 cells with 20 μM cytochalasin B induced G2/M cell cycle arrest (63.72%) without significant cell death. Treatment of HepG2 cells with 200 μM Ph increased the sub-G1 population to 22.54%, indicating significant cell death. Combined treatment of HepG2 cells with 200 μM Ph and 0.5–20 μM cytochalasin B increased the sub-G1 population from 30.76 to 70.37% in a dose-dependent fashion, indicating enhancement of cell death. To test whether cytochalasin B enhancement of Ph-induced HepG2 cell death was associated with glucose transport interference, a flow cytometry study (Fig. 4*b*) was performed. Combined treatment of HepG2 cells with 200 μM Ph and 20 μM cytochalasin B increased the sub-G1 population from 23.04 to 68.85%; this population was reduced to 7.53% by treatment with 100 mM glucose. These findings indicate that cytochalasin B enhancement of Ph-induced HepG2 apoptosis involves perturbation of glucose transport.

Decreased $\Delta\Psi_m$ has been linked to apoptotic cell death. To determine the effects of Ph and cytochalasin B on the $\Delta\Psi_m$ change in apoptotic HepG2 cells, flow cytometry analysis was performed. HepG2 cells were stained with a cationic lipophilic fluorescent dye, JC-1, which emits red or green light in response to a high or low $\Delta\Psi_m$, respectively. Therefore, the mitochondrial membrane potential can be measured by the red/green fluorescence intensity ratio. As shown in Figure 4*c*, treatment of HepG2 cells with 20 μM cytochalasin B for 24 hr showed no significant $\Delta\Psi_m$ change compared with the control. Treatment of HepG2 cells with 200 μM Ph for 24 hr caused a significant decrease in $\Delta\Psi_m$, evidenced by a shift from red (FL2) to green (FL1) fluorescence. Combined treatment of HepG2 cells with 200 μM Ph and 20 μM cytochalasin B further decreased $\Delta\Psi_m$. Cotreatment with 100 mM glucose reversed the cytochalasin B enhancement of the Ph-induced decrease of $\Delta\Psi_m$ in HepG2 cells. These findings indicate that cytochalasin B enhancement of the Ph-induced decrease in $\Delta\Psi_m$ of HepG2 cells involves regulation of glucose transport.

To verify that the cytochalasin B enhancement of Ph-induced HepG2 cell death involved glucose transport, Western blot studies of apoptotic regulatory proteins were performed. As shown in Figure 4*d*, treatment of HepG2 cells with 20 μM cytochalasin B did not activate caspases or apoptotic regulatory proteins. However, treatment of HepG2 cells with 200 μM Ph activated caspases 3, 8 and 9, along with increased expression of p53 protein, translocation of Bax from the cytosol to the mitochondria, decreased expression of Bcl-2 protein, formation of truncated Bid and translocation of cytochrome c from the mitochondria to the cytosol. This treatment also led to inhibition of Akt phosphorylation, Bad translocation from the cytosol to mitochondria, suppression of XIAP and survivin expression, and AIF translocation from the mitochondria to the nucleus. Combined treatment of HepG2 cells with 200 μM Ph and 20 μM cytochalasin B further enhanced the activation of caspases 3, 8 and 9, and increased both the expression of p53 protein and the translocation of Bax from the cytosol to the mitochondria. This treatment also decreased expression of Bcl-2 protein, formation of truncated Bid and translocation of cytochrome c from the mitochondria to the cytosol. All of these effects were reversed by cotreatment with 100 mM glucose.

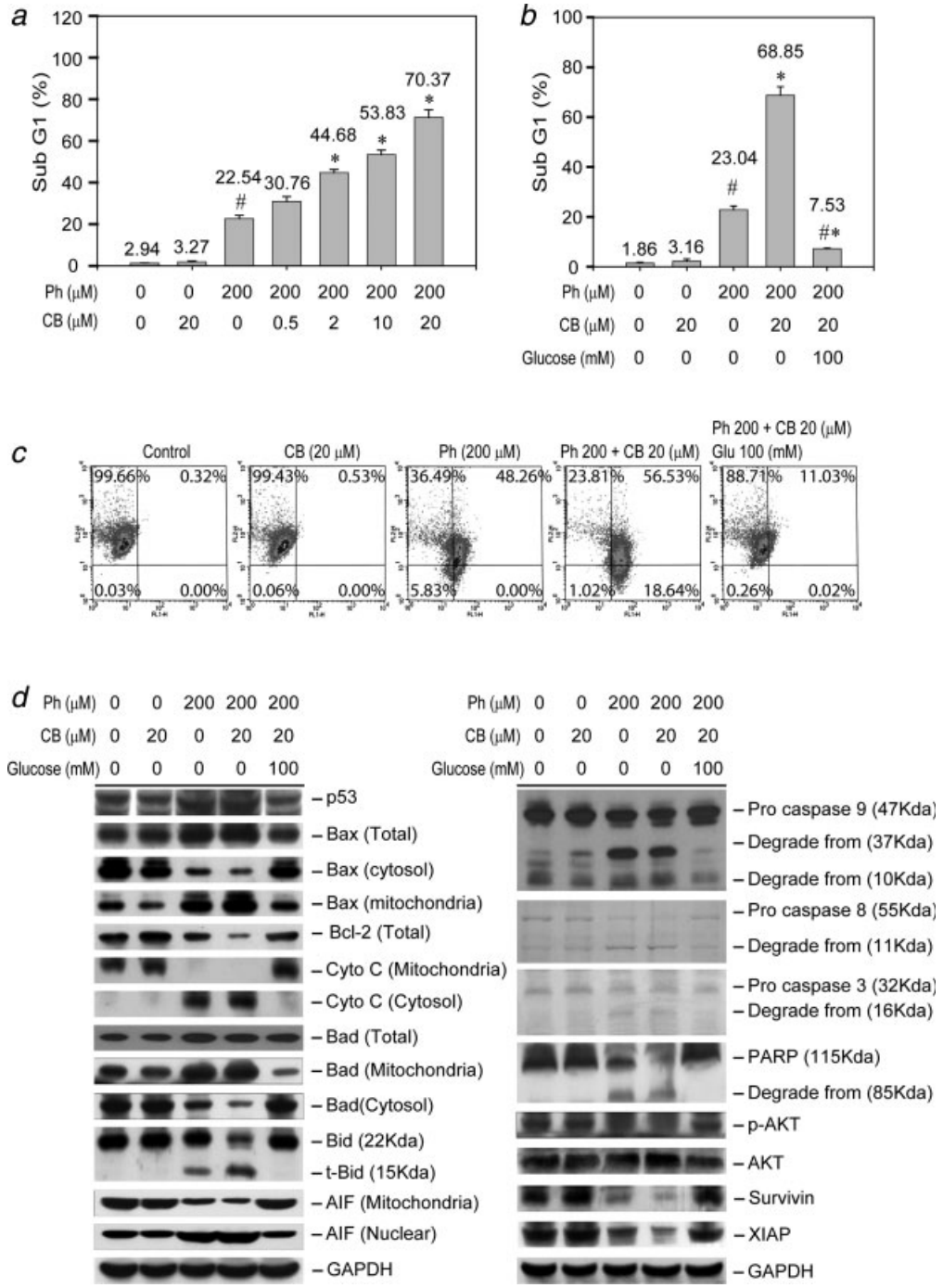

Figure 4 – Effects of cytochalasin B (CB) on Ph-induced apoptosis in HepG2 cells. (*a*) FACS analysis of the subG1 percentage was conducted after HepG2 cells were incubated for 24 hr in culture medium supplemented with 10% FCS and 0.05% DMSO, with or without Ph (200 and 0 μM), and with various concentrations of CB (0–20 μM). Three samples were analyzed in each group, and values are presented as means ± SE.[#], $p < 0.05$ *vs*. DMSO (0 μM of Ph) control; *, $p < 0.05$ *vs*. 200 μM Ph. (*b*) FACS analysis of the subG1 percentage was conducted after HepG2 cells were incubated for 24 hr in culture medium supplemented with 10% FCS and 0.05% DMSO, with or without Ph (200 and 0 μM), with or without CB (20 or 0 μM), and with or without glucose (100 or 0 mM). Three samples were analyzed in each group, and the resulting values are presented as means ± SE.[#], $p < 0.05$ *vs*. DMSO (0 μM of Ph) control; *, $p < 0.05$ *vs*. 200 μM Ph;[#]*, $p < 0.05$ *vs*. 200 μM Ph and 20 μM CB plus 200 μM Ph (*c*) FACS analysis of HepG2 mitochondrial membrane potential changes measured by JC-1 staining. Cells were incubated for 24 hr in culture medium supplemented with 10% FCS and 0.05% DMSO and the following additions: no Ph, CB, or glucose; only Ph (200 μM) and CB (20 μM); both Ph (200 μM) and CB (20 μM); and Ph (200 μM), CB (20 μM), and glucose (100 mM). Results are expressed as percent change from red (FL2) to green (FL1) fluorescence. (*d*) Effects of CB on Ph-induced activation of apoptotic regulatory proteins and the reversibility of these effects with glucose in HepG2 cells. The cells were incubated for 24 hr in culture medium supplemented with 10% FCS and 0.05% DMSO with or without Ph (200 and 0 μM), with or without CB (20 or 0 μM), and with or without glucose (100 or 0 mM).

Ph inhibition of HepG2 xenograft growth in mice involves suppression of glucose uptake

We further examined the antitumor effect of Ph *in vivo* by treating SCID mice bearing HepG2 tumor xenografts. After growth of palpable tumors (mean tumor volume, 200 mm^3), animals received Ph at a dose of 10 mg/kg or DMSO control 3 times per week. The tumor size of Ph-treated group began to decrease significantly compared with control group from the second to the sixth week (Fig. 5*a*), and the final tumor weight (Fig. 5*b*) was significantly smaller in Ph-treated group than in control group. In mice receiving these treatment regimens, no gross signs of toxicity were observed based on body weight, visible inspection of general appearance or microscopic examination of individual organs (data not shown). To determine whether Ph-induced suppression of liver tumor growth involved regulation of glucose transport, an ^{18}F-FDG microPET study was performed. As shown in Figure 5*c*, ^{18}F-FDG uptake in the Ph-treated HepG2 tumor-bearing mice was significantly suppressed relative to control mice. With microPET analysis in these mice, tumor volumes were significantly smaller in the Ph-treated groups compared to controls (Fig. 5*d*). After intravenous injection of the same dosage of ^{18}F-FDG into Ph-treated and control mice (Fig. 5*e*), quantitative tumor uptake decreased ~10-fold in the Ph-treated, tumor-bearing mice compared to the control mice (Fig. 5*f*). These findings suggest that suppression of glucose uptake into tumor tissues is involved in the Ph-induced inhibition of hepatoma xenograft growth in mice.

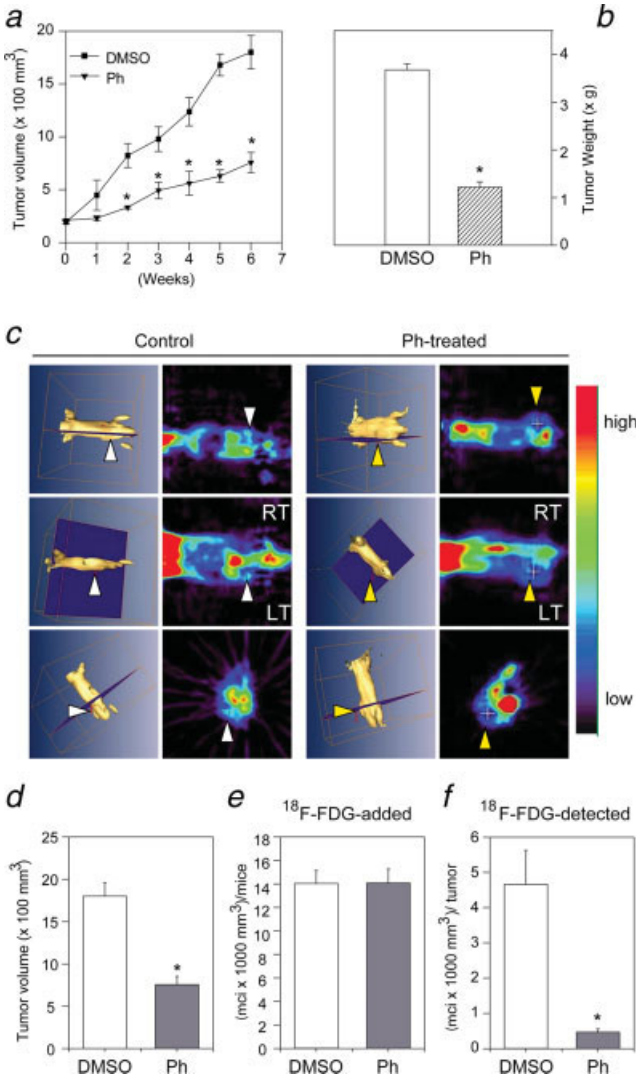

FIGURE 5 – The growth of HepG2 tumor xenografts in SCID mice was suppressed by Ph treatment, and this involved suppression of glucose uptake visualized by microPET analysis. SCID mice were injected with HepG2 cells in the subcutaneous tissue of the interscapular area. Once tumor volume reached ~200 mm^3, animals were treated intraperitoneally with 10 mg/kg Ph or DMSO, 3 times per week for 6 weeks. (*a*) Average tumor volume of DMSO-treated (square, $n = 5$) *vs*. Ph-treated (triangle, $n = 5$) SCID mice. (*b*) Tumor weight was measured at the end of the experiment. (*c*) ^{18}F-FDG microPET study of control and Ph-treated mice. A three-dimensional study was performed. The color chart on the right panel indicates the intensity of glucose uptake. The arrowhead indicates the location of the tumor. RT, right; LT, left. (*d*) Tumor volumes of control and Ph-treated mice in the microPET study. (*e*) ^{18}F-FDG injection into the control and Ph-treated mice. (*f*) Comparison of quantitative uptake of ^{18}F-FDG in tumors between the DMSO and Ph-treated tumor-bearing mice. Five samples were analyzed in each group, and values represent the means ± SE. *Significant difference at $p < 0.05$.

Discussion

An increased rate of glucose uptake into the transformed cells is one of the alterations of cellular function that occurs when the sarcoma virus transforms normal cells into malignant cells.[33] The elevated glucose transport into malignant cells is associated with increased expression of GLUTs.[11] Positron emission tomography has been used to show that high-grade tumors take up more FDG than low-grade tumors, and this increased uptake is associated with more aggressive behavior and poor prognosis.[34,35] Suppressing glucose uptake by tumors, therefore, is a reasonable strategy to pursue in the search for improved cancer therapies. Our cellular and animal studies clearly show that Ph selectively suppresses hepatoma cell growth by activating apoptosis through inhibition of glucose transport mechanisms. To our knowledge, this is the first demonstration that Ph exerts an antitumor effect on hepatoma cells both *in vitro* and *in vivo*.

Ph has been shown to stimulate transcriptional activity of the human estrogen receptor and to compete for the binding of radiolabeled 17β-estradiol to this protein,[36] suggesting that Ph can act as a nonsteroid estrogen. However, previous reports have demonstrated that treatment of HepG2 cells with 17β-estradiol induces cell proliferation,[37] suggesting that the potential effect of Ph on the estrogen receptor is not involved in Ph-induced cell death in HepG2 cells. Ph has been shown to suppress the protein kinase C (PKC) pathway in melanoma cells. The effects on HepG2 cells of modulating PKC pathways are complex.[38] Nevertheless, it is clear from the present work that pretreatment with glucose reverses the apoptotic effect of Ph on HepG2 cells and that siRNA knockdown of GLUT2 expression induced HepG2 cell apoptosis which cannot be reversed by glucose treatment suggesting a direct involvement of GLUT2 in the Ph-induced cytotoxicity in liver cancer cells.

In our study, 200 μM Ph was used to induce HepG2 cell apoptosis. Using primary rat hepatocytes, previous reports demonstrated that Ph at 0.4 to 200 μM significantly reduced tert-butyl hydroperoxide-induced cytotoxicity,[39] and reported that the LD_{50} of Ph is 500 ± 51 μM.[40] One report showed that Ph at 30 μM protected Aβ peptide-induced plasma membrane damage in PC12 cells, while 300 μM Ph became toxic to the cells.[41] Ph at 50 to 500 μM blocked *Helicobacter pylori* cytotoxin VacA-mediated urea/ion transport and the toxin's major biological effects.[42] Importantly, Ph of 10 mg/kg in our *in vivo* HepG2 xenograft mice model showed significant antitumor effects without apparent toxicity. This dosage of Ph has been reported to be nontoxic in animal study using female rats.[43] These data suggest that the doses of Ph used in our *in vitro* and *in vivo* studies on hepatoma cells might be feasible approaches.

Malignant cells have an increased metabolic rate.[11] Furthermore, the activity of lactate dehydrogenase[44] and pentose phosphate pathway enzymes[45,46] is increased in malignant cells. These changes mean that a reduced amount of pyruvate is available to mitochondria, resulting in a low oxidation rate *via* the tricarbox-

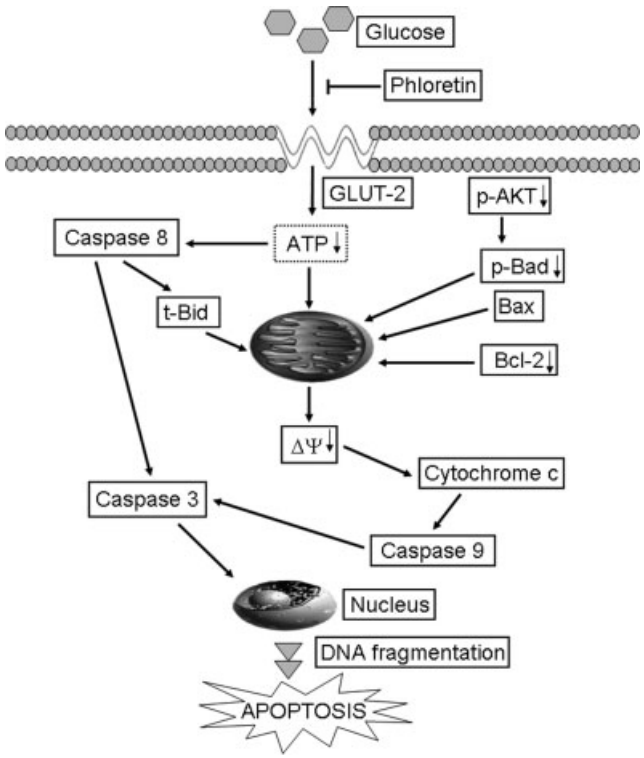

FIGURE 6 – Mode of phloretin-induced apoptosis on human liver cancer cells. In response to phloretin treatment, cell glucose uptake is suppressed involving type II glucose transporter. Subsequently, suppression of ATP production results in mitochondrial membrane potential breakdown and activation of both intrinsic and extrinsic apoptotic signaling pathways, which, in turn, induce apoptosis of live cancer cells.

ylic acid cycle.[45] The high energy requirements of tumors, together with their low energy production, leads to an increased rate of glycolysis and, therefore, glucose uptake. These observations are compatible with our findings that both human hepatoma cells and HCC tissue show increased expression of GLUT2 in the cell membrane.

ATP depletion is an important mechanism of apoptosis.[22,47] Mitochondrial membrane potential, the driving force of ATP production, is decreased during apoptosis.[48] Partial ATP depletion induced the activation of the caspase 8-associated extrinsic apoptotic pathways in kidney cells.[49] Our results show that Ph induces apoptosis in hepatoma cells by inhibiting glucose transport, and subsequently by the possible suppression of ATP production, resulting in mitochondrial membrane potential reduction (Fig. 6). Both intrinsic and extrinsic apoptotic pathways are implicated in this study, which may reflect the fact that 200 μM Ph causes more severe ATP depletion[23] and, therefore, leads to the breakdown of mitochondria, activating downstream apoptotic pathways.

Elevation of facilitated glucose transporter mRNA in human HCC has been demonstrated using northern blot analysis.[50] In a study of various human gastrointestinal cancers, GLUT2 mRNA was primarily restricted to the liver, with increased expression of GLUT2 transcripts in tumorous *vs.* normal tissues.[20] In contrast, GLUT2 expression was reduced in hepatic preneoplastic or neoplastic lesions, with expression of GLUT1 in HCC.[51] However, no expression of GLUT1 has been reported in human HCC or nontumorous tissues.[21] Our results showed significantly increased expression of GLUT2 protein in human HCC and hepatoma cells in the cell membrane, suggesting translocation of the protein.[24,52,53] The difference between our results and those of Grobholz *et al*.[51] may be that they used an animal model of chemically induced hepatocarcinogenesis (*N*-nitrosomorpholine) rather than the human HCC tumor model used in other studies.

On the basis of our results, we propose a model for the molecular mechanism of Ph-induced apoptosis on HepG2 cells (Fig. 6). Our experimental findings demonstrate that Ph, a naturally occurring compound with glucose transporter inhibitory activity, exerts antitumor activity through the induction of apoptosis in hepatoma cells both in culture and in tumor-bearing SCID mice. The results of these *in vitro* and *in vivo* studies shed light on the molecular mechanisms of selective Ph-induced cytotoxicity in hepatoma cells. These findings may have potential applications in the treatment of liver cancer.

Acknowledgements

This work was supported by research grants from the National Science Council of Taiwan to Dr. Ho, Dr. Wu and Dr. Lin. Technical support was obtained from Molecular and Genetic Imaging Core/NRPGM.

References

1. Le Marchand L, Murphy SP, Hankin JH, Wilkens LR, Kolonel LN. Intake of flavonoids and lung cancer. J Natl Cancer Inst 2000;92:154–60.
2. Boyer J, Liu RH. Apple phytochemicals and their health benefits. Nutr J 2004;3:5.
3. Eberhardt MV, Lee CY, Liu RH. Antioxidant activity of fresh apples. Nature 2000;405:903–4.
4. He X, Liu RH. Triterpenoids isolated from apple peels have potent antiproliferative activity and may be partially responsible for apple's anticancer activity. J Agric Food Chem 2007;55:4366–70.
5. Yoon H, Liu RH. Effect of selected phytochemicals and apple extracts on NF-kappaB activation in human breast cancer MCF-7 cells. J Agric Food Chem 2007;55:3167–73.
6. Kobori M, Shinmoto H, Tsushida T, Shinohara K. Phloretin-induced apoptosis in B16 melanoma 4A5 cells by inhibition of glucose transmembrane transport. Cancer Lett 1997;119:207–12.
7. Salter DW, Custead-Jones S, Cook JS. Quercetin inhibits hexose transport in a human diploid fibroblast. J Membr Biol 1978;40:67–76.
8. Gschwendt M, Horn F, Kittstein W, Furstenberger G, Besemfelder E, Marks F. Calcium and phospholipid-dependent protein kinase activity in mouse epidermis cytosol. Stimulation by complete and incomplete tumor promoters and inhibition by various compounds. Biochem Biophys Res Commun 1984;124:63–8.
9. Devi MA, Das NP. In vitro effects of natural plant polyphenols on the proliferation of normal and abnormal human lymphocytes and their secretions of interleukin-2. Cancer Lett 1993;69:191–6.
10. Nelson JA, Falk RE. The efficacy of phloridzin and phloretin on tumor cell growth. Anticancer Res 1993;13:2287–92.
11. Macheda ML, Rogers S, Best JD. Molecular and cellular regulation of glucose transporter (GLUT) proteins in cancer. J Cell Physiol 2005;202:654–62.
12. Joost HG, Thorens B. The extended GLUT-family of sugar/polyol transport facilitators: nomenclature, sequence characteristics, and potential function of its novel members (review). Mol Membr Biol 2001;18:247–56.
13. Gould GW, Bell GI. Facilitative glucose transporters: an expanding family. Trends Biochem Sci 1990;15:18–23.
14. Fukumoto H, Seino S, Imura H, Seino Y, Eddy RL, Fukushima Y, Byers MG, Shows TB, Bell GI. Sequence, tissue distribution, and chromosomal localization of mRNA encoding a human glucose transporter-like protein. Proc Natl Acad Sci USA 1988;85:5434–8.
15. Thorens B, Sarkar HK, Kaback HR, Lodish HF. Cloning and functional expression in bacteria of a novel glucose transporter present in liver, intestine, kidney, and beta-pancreatic islet cells. Cell 1988;55:281–90.
16. Hennipman A, Smits J, van Oirschot B, van Houwelingen JC, Rijksen G, Neyt JP, Van Unnik JA, Staal GE. Glycolytic enzymes in breast cancer, benign breast disease and normal breast tissue. Tumour Biol 1987;8:251–63.
17. Lee JD, Yang WI, Park YN, Kim KS, Choi JS, Yun M, Ko D, Kim TS, Cho AE, Kim HM, Han KH, Im SS, et al. Different glucose uptake and glycolytic mechanisms between hepatocellular carcinoma

and intrahepatic mass-forming cholangiocarcinoma with increased (18)F-FDG uptake. J Nucl Med 2005;46:1753–9.
18. Khan MA, Combs CS, Brunt EM, Lowe VJ, Wolverson MK, Solomon H, Collins BT, Di Bisceglie AM. Positron emission tomography scanning in the evaluation of hepatocellular carcinoma. J Hepatol 2000;32:792–7.
19. Torizuka T, Tamaki N, Inokuma T, Magata Y, Sasayama S, Yonekura Y, Tanaka A, Yamaoka Y, Yamamoto K, Konishi J. In vivo assessment of glucose metabolism in hepatocellular carcinoma with FDG-PET. J Nucl Med 1995;36:1811–7.
20. Yamamoto T, Seino Y, Fukumoto H, Koh G, Yano H, Inagaki N, Yamada Y, Inoue K, Manabe T, Imura H. Over-expression of facilitative glucose transporter genes in human cancer. Biochem Biophys Res Commun 1990;170:223–30.
21. Younes M, Lechago LV, Somoano JR, Mosharaf M, Lechago J. Wide expression of the human erythrocyte glucose transporter Glut1 in human cancers. Cancer Res 1996;56:1164–7.
22. Moley KH, Mueckler MM. Glucose transport and apoptosis. Apoptosis 2000;5:99–105.
23. Jordan NJ, Holman GD. Photolabelling of the liver-type glucose-transporter isoform GLUT2 with an azitrifluoroethylbenzoyl-substituted bis-D-mannose. Biochem J 1992;286 (Part 2):649–56.
24. Walker J, Jijon HB, Diaz H, Salehi P, Churchill T, Madsen KL. 5-aminoimidazole-4-carboxamide riboside (AICAR) enhances GLUT2-dependent jejunal glucose transport: a possible role for AMPK. Biochem J 2005;385:485–91.
25. Lee WS, Chen RJ, Wang YJ, Tseng H, Jeng JH, Lin SY, Liang YC, Chen CH, Lin CH, Lin JK, Ho PY, Chu JS, et al. In vitro and in vivo studies of the anticancer action of terbinafine in human cancer cell lines: G0/G1 p53-associated cell cycle arrest. Int J Cancer 2003;106:125–37.
26. Ho YS, Wu CH, Chou HM, Wang YJ, Tseng H, Chen CH, Chen LC, Lee CH, Lin SY. Molecular mechanisms of econazole-induced toxicity on human colon cancer cells: G0/G1 cell cycle arrest and caspase 8-independent apoptotic signaling pathways. Food Chem Toxicol 2005;43:1483–95.
27. Wang SK, Liang PH, Astronomo RD, Hsu TL, Hsieh SL, Burton DR, Wong CH. Targeting the carbohydrates on HIV-1: interaction of oligomannose dendrons with human monoclonal antibody 2G12 and DC-SIGN. Proc Natl Acad Sci USA 2008;105:3690–5.
28. Yang KC, Wu CC, Wu CH, Chen JH, Chu CH, Chen CH, Chou YH, Wang YJ, Lee WS, Tseng H, Lin SY, Lee CH, et al. Involvement of proapoptotic Bcl-2 family members in terbinafine-induced mitochondrial dysfunction and apoptosis in HL60 cells. Food Chem Toxicol 2006;44:214–26.
29. Osborne CK, Coronado EB, Robinson JP. Human breast cancer in the athymic nude mouse: cytostatic effects of long-term antiestrogen therapy. Eur J Cancer Clin Oncol 1987;23:1189–96.
30. Wang HE, Wu SY, Chang CW, Liu RS, Hwang LC, Lee TW, Chen JC, Hwang JJ. Evaluation of F-18-labeled amino acid derivatives and [18F]FDG as PET probes in a brain tumor-bearing animal model. Nucl Med Biol 2005;32:367–75.
31. Thornberry NA, Lazebnik Y. Caspases: enemies within. Science 1998;281:1312–6.
32. Axelrod JD, Pilch PF. Unique cytochalasin B binding characteristics of the hepatic glucose carrier. Biochemistry 1983;22:2222–7.
33. Hatanaka M. Transport of sugars in tumor cell membranes. Biochim Biophys Acta 1974;355:77–104.
34. Oshida M, Uno K, Suzuki M, Nagashima T, Hashimoto H, Yagata H, Shishikura T, Imazeki K, Nakajima N. Predicting the prognoses of breast carcinoma patients with positron emission tomography using 2-deoxy-2-fluoro[18F]-D-glucose. Cancer 1998;82:2227–34.
35. Halfpenny W, Hain SF, Biassoni L, Maisey MN, Sherman JA, McGurk M. FDG-PET. A possible prognostic factor in head and neck cancer. Br J Cancer 2002;86:512–6.
36. Miksicek RJ. Interaction of naturally occurring nonsteroidal estrogens with expressed recombinant human estrogen receptor. J Steroid Biochem Mol Biol 1994;49:153–60.
37. Marino M, Acconcia F, Bresciani F, Weisz A, Trentalance A. Distinct nongenomic signal transduction pathways controlled by 17beta-estradiol regulate DNA synthesis and cyclin D(1) gene transcription in HepG2 cells. Mol Biol Cell 2002;13:3720–9.
38. Wen-Sheng W, Jun-Ming H. Activation of protein kinase C alpha is required for TPA-triggered ERK (MAPK) signaling and growth inhibition of human hepatoma cell HepG2. J Biomed Sci 2005;12:289–96.
39. An RB, Park EJ, Jeong GS, Sohn DH, Kim YC. Cytoprotective constituent of Hoveniae Lignum on both Hep G2 cells and rat primary hepatocytes. Arch Pharm Res 2007;30:674–7.
40. Moridani MY, Galati G, O'Brien PJ. Comparative quantitative structure toxicity relationships for flavonoids evaluated in isolated rat hepatocytes and HeLa tumor cells. Chem Biol Interact 2002;139:251–64.
41. Hertel C, Terzi E, Hauser N, Jakob-Rotne R, Seelig J, Kemp JA. Inhibition of the electrostatic interaction between beta-amyloid peptide and membranes prevents beta-amyloid-induced toxicity. Proc Natl Acad Sci USA 1997;94:9412–6.
42. Tombola F, Morbiato L, Del Giudice G, Rappuoli R, Zoratti M, Papini E. The Helicobacter pylori VacA toxin is a urea permease that promotes urea diffusion across epithelia. J Clin Invest 2001;108:929–37.
43. Nelson JA, Falk RE. Phloridzin and phloretin inhibition of 2-deoxy-D-glucose uptake by tumor cells in vitro and in vivo. Anticancer Res 1993;13:2293–9.
44. Shim H, Dolde C, Lewis BC, Wu CS, Dang G, Jungmann RA, Dalla-Favera R, Dang CV. c-Myc transactivation of LDH-A: implications for tumor metabolism and growth. Proc Natl Acad Sci USA 1997;94:6658–63.
45. Board M, Humm S, Newsholme EA. Maximum activities of key enzymes of glycolysis, glutaminolysis, pentose phosphate pathway and tricarboxylic acid cycle in normal, neoplastic and suppressed cells. Biochem J 1990;265:503–9.
46. Ikezaki K, Black KL, Conklin SG, Becker DP. Histochemical evaluation of energy metabolism in rat glioma. Neurol Res 1992;14:289–93.
47. Nakamura N, Wada Y. Properties of DNA fragmentation activity generated by ATP depletion. Cell Death Differ 2000;7:477–84.
48. Richter C, Schweizer M, Cossarizza A, Franceschi C. Control of apoptosis by the cellular ATP level. FEBS Lett 1996;378:107–10.
49. Feldenberg LR, Thevananther S, del Rio M, de Leon M, Devarajan P. Partial ATP depletion induces Fas- and caspase-mediated apoptosis in MDCK cells. Am J Physiol 1999;276:F837–F46.
50. Su TS, Tsai TF, Chi CW, Han SH, Chou CK. Elevation of facilitated glucose-transporter messenger RNA in human hepatocellular carcinoma. Hepatology 1990;11:118–22.
51. Grobholz R, Hacker HJ, Thorens B, Bannasch P. Reduction in the expression of glucose transporter protein GLUT 2 in preneoplastic and neoplastic hepatic lesions and reexpression of GLUT 1 in late stages of hepatocarcinogenesis. Cancer Res 1993;53:4204–11.
52. Reimer MK, Ahren B. Altered beta-cell distribution of pdx-1 and GLUT-2 after a short-term challenge with a high-fat diet in C57BL/6J mice. Diabetes 2002;51(Suppl 1):S138–S43.
53. Bogan JS, Hendon N, McKee AE, Tsao TS, Lodish HF. Functional cloning of TUG as a regulator of GLUT4 glucose transporter trafficking. Nature 2003;425:727–33.